JOURNAL OF SOLID STATE CHEMISTRY 117, 386–391 (1995)

Structure and Properties of Hydrothermally Synthesized Thiosulfate Cancrinite

G.-G. Lindner, W. Massa, and D. Reinen[1]

Fachbereich Chemie und Zentrum für Materialwissenschaften der Philipps-Universität Marburg, Hans-Meerweinstrasse, D-35032 Marburg, Germany

Received September 16, 1994; accepted December 19, 1994

Thiosulfate cancrinite was prepared by hydrothermal methods. The single crystal *X*-ray investigation yielded the space group *P*3 (a = 12.624(2) Å, c = 5.170(1) Å, R = 0.031, at 193 K). Axial twinning along [001] was observed. The thiosulfate anions show orientational disorder. On irradiation or heating, yellow to greenish-blue coloration occurs according to the formation of S_2^- and S_3^- radicals within the spacy channels of the cancrinite structure. These radicals are identified by UV/VIS and ESR spectroscopy, and a mechanism of formation is proposed. © 1995 Academic Press, Inc.

I. INTRODUCTION

Similar to sodalite-type zeolites like ultramarines (1, 2), aluminosilicates of the cancrinite-type attract attention due to coloration phenomena by entrapped chalcogen radicals. In the cancrinite family, the ordered aluminosilicate framework of the idealized composition $[Al_6Si_6O_{24}]^{6-}$ has a channel structure (Fig. 1) which may include additional Na^+ cations, anions, and water, approaching stoichiometries such as $Na_8[Al_6Si_6O_{24}]X^n_{2/n} \cdot mH_2O$. As anions, sulfate, carbonate, nitrate, nitrite, chlorate, and thiosulfate have been reported (3–11). Single crystal structure investigations, e.g., performed with sulfate and carbonate (4, 5, 10, 11), yielded the space group $P6_3$. In the case of the thiosulfate cancrinite, only powders have been investigated thus far (3). We succeeded in growing single crystals large enough for a single crystal structure determination by hydrothermal methods (Fig. 2). The structure investigation reveals a lower symmetry cancrinite variant, and we further report the results of subsequent irradiation and thermal treatments yielding colored species.

II. EXPERIMENTAL

II.1. Sample Preparation

Sodium aluminate (1.135 g), NaOH (11.25 g), and $Na_2S_2O_3 \cdot 5H_2O$ (20 g) were dissolved in 35.5 ml water. Three milliliters water glass (37–40%) in 5 ml water was added slowly while stirring. A platinum-lined autoclave was filled up to 60% with the resulting gel and held for 28 days at 300°C (autogenous pressure about 85 bar). The resulting colorless crystalline substance was washed thoroughly with water and dried at 80°C.

II.2. Chemical Analysis

Because only a small amount of compound was available, the chemical analysis was performed by energy-dispersive scanning electron microscopy (Joel JSM-6400, 15 kV) and yielded the following composition (averaged over five measurements; sulfur was assumed to be present as thiosulfate):

$$Na_{6.9\pm0.2}[Al_{5.6\pm0.1}Si_{6.4\pm0.1}O_{24}](S_2O_3)_{1\pm0.1} \cdot nH_2O.$$

The experimental density D_m = 2.39 g/ml compares well with the theoretical density D_x = 2.43 g/ml of the dihydrate (n = 2). The low sodium content contrasts with the value of ≈7.6 expected for charge balance and is attributed to a systematic error. The rather high energy concentration during the SEM measurement apparently causes sodium to partly "evaporate" as is confirmed by the decrease in the sodium content with irradiation time. The X-ray structure determination (III.1) yields fully occupied sodium positions. Because the refinement is very sensitive to the electron-rich sodium ions, the Na^+ content can be assumed to approach nearly 8.

II.3. ESR Measurements and UV/VIS Spectroscopy

Electron spin resonance measurements were performed with a Bruker ESP 300E spectrometer. The UV/VIS spectra were obtained with a Hitachi U-3410 UV/VIS/NIR spectrophotometer with an integrating sphere attachment (Ulbricht-Kugel) under conditions of diffuse reflectance.

II.4. X-Ray Diffraction Analysis

The X-ray investigations were carried out with a Weissenberg camera and a NONIUS CAD-4 four-circle diffrac-

[1] To whom correspondence should be addressed.

0022-4596/95 $12.00

TABLE 1
Crystal Data and Structure Refinement

Empirical formula	$Na_8[Al_6Si_6O_{24}]S_2O_3 \cdot 2H_2O$
Formula weight	1046.49
Temperature	193 K (−80°C)
Wavelength	1.54178 Å
Crystal system	Trigonal
Space group	*P*3 (No. 143)
Unit cell dimensions	a = 12.624(2) Å c = 5.170(1) Å
Volume	713.5(2) Å^3
Z	1
Density (calculated)	2.435 g/ml
Absorption coefficient	8.271 mm^{-1}, numerical corr.
F(000)	518
Crystal size	0.038 × 0.038 × 0.54 mm
Theta range for data collection	4.0 to 78.4°
Index ranges	$-15 \le h \le 8, 0 \le k \le 16, 0 \le l \le 5$
Reflections collected	3273
Independent reflections	1098
Refinement method	Full-matrix least-squares on F^2 (12)
Scattering factors, $\Delta f'$, $\Delta f''$	(13)
Parameters	116
Goodness-of-fit on F^2	1.122
Residuals	
$[I > 2\sigma(I)]$	R = 0.0307, wR_2 = 0.0725
[all data]	R = 0.0352, wR_2 = 0.0759
Extinction coefficient	0.0032(4)
Largest diff. peak and hole	0.386 and −0.497 $e \cdot$ Å^{-3}

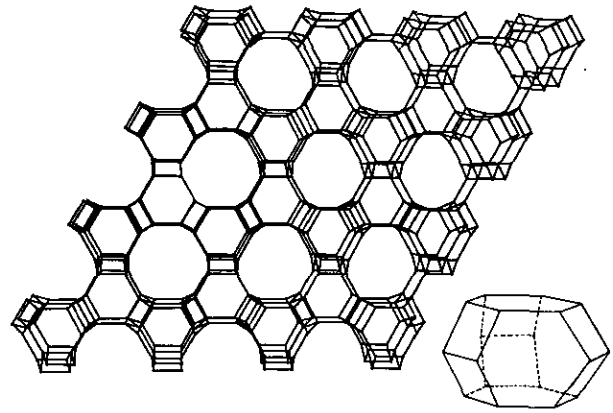

FIG. 1. Schematic view of the cancrinite channel structure and the ε-cage (undecahedral cage) from which the framework is built.

tometer (Cu$K\alpha$) at −80°C. The crystal data and experimental conditions are compiled in Table 1.

III. RESULTS AND DISCUSSION

III.1. Structure

The unit cell dimensions refined from 25 high angle reflections recorded at the diffractometer are a = 12.624(2) Å and c = 5.170(1) Å at −80°C, slightly lower

TABLE 2
Wyckhoff Positions, Atomic Coordinates (×10^4), Occupation Factors *K*, and Equivalent Isotropic Displacement Parameters (Å^2 × 10^3) of $Na_8[Al_6Si_6O_{24}](S_2O_3) \cdot 2H_2O$

		x	*y*	*z*	*K*	U_{eq}
Al(1)	3*d*	9258(3)	5869(3)	2240	1.00	7(1)
Al(2)	3*d*	769(3)	4134(3)	7195(14)	1.00	7(1)
Si(1)	3*d*	6711(2)	5892(3)	2273(15)	1.00	7(1)
Si(2)	3*d*	3288(2)	4128(3)	7184(9)	1.00	7(1)
O(11)	3*d*	7970(7)	5946(5)	3083(20)	1.00	13(1)
O(12)	3*d*	2021(7)	4017(6)	8148(19)	1.00	13(1)
O(21)	3*d*	8834(6)	4349(7)	2739(18)	1.00	14(1)
O(22)	3*d*	1211(6)	5664(6)	7213(20)	1.00	14(1)
O(31)	3*d*	9696(7)	6391(7)	9133(19)	1.00	12(1)
O(32)	3*d*	271(7)	3452(7)	4154(19)	1.00	12(1)
O(41)	3*d*	6748(6)	6340(7)	9333(18)	1.00	13(1)
O(42)	3*d*	3119(6)	3556(7)	4323(19)	1.00	13(1)
Na(11)	1*b*	1/3	2/3	8551(24)	1.00	23(1)
Na(12)	1*b*	2/3	1/3	3474(19)	1.00	23(1)
Na(21)	3*d*	8662(4)	7214(4)	6932(14)	1.00	23(1)
Na(22)	3*d*	1284(4)	2601(4)	1825(13)	1.00	23(1)
O(51)	3*d*	6910(37)	3039(36)	7821(53)	1.00	38(4)
O(52)	3*d*	3158(45)	6909(42)	3037(52)	1.00	38(4)
S(1)	1*a*	0	0	8919	1.00	53(2)
S(2)/O(2)	1*a*	0	0	5636(33)	0.3/0.3	48(4)
S(3)/O(3)	3*d*	9352(9)	628(11)	2362(59)	0.1/0.5	48(4)
S(4)/(O4)	1*a*	0	0	2362(59)	0.2/0.2	48(4)
S(5)/O(5)	3*d*	8725(13)	9324(16)	7675(51)	0.067/0.333	64(3)

Note. U_{eq} is defined as one-third of the trace of the orthogonalized U_{ij} tensor.

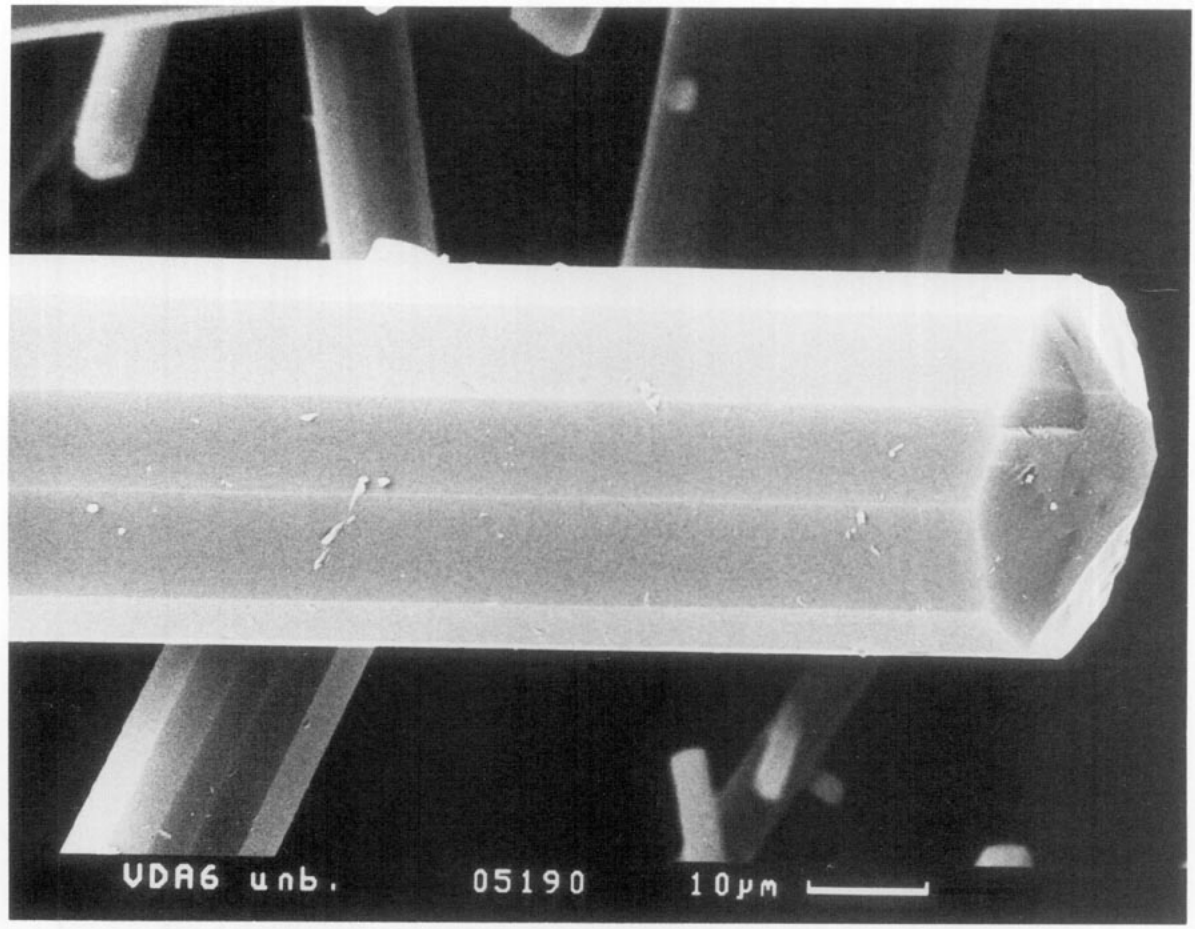

FIG. 2. SEM image of a thiosulfate cancrinite crystal.

than at room temperature: a = 12.656(2) Å and c = 5.164(1) Å. These values are in good agreement with those found by Hund (3) and Barrer (4) for powder samples of thiosulfate cancrinite. No superstructure reflections or other anomalies were detected in the film records. The Laue group appeared to be $6/m$, but the systematic extinction rule for (001): $1 \neq 2n$ is not obeyed. Renninger effects or $\lambda/2$ contributions could be excluded as possible reasons. Thus, the usual space group $P6_3$ for cancrinites cannot be used nor any other hexagonal space group belonging to the low Laue class, because they are not compatible with the topology of the cancrinite framework. The structure was described, therefore, in the maximal subgroup $P3$, which allows for the presence of only *one* $S_2O_3^{2-}$ anion per unit cell. In the space group $P6_3$ the presence of a 6_3-axis in the channel center would generate *two* equivalent groups stacked by a $c/2$ translation, implying an unrealistically short distance of 2.585 Å between the centers of the two $S_2O_3^{2-}$ anions. The experimental results—the reflections showed perfect hexagonal Laue symmetry in spite of the need to adopt a trigonal space group—hence suggest twinning by merohedry. In fact, using the twin law of an axial [001] twin, a structural model including the $[Al_6Si_6O_{24}]$ framework and eight sodium ions could be refined with reasonable results. Subsequent difference Fourier syntheses revealed electron densities attributable to disordered crystal water and thiosulfate anions. The positional parameters of the constituting atoms and selected bond distances and angles are given in Tables 2 and 3. A view of the structure along the [001] direction is depicted in Fig. 3.

After testing various split-atom models for the distribution and orientation of the $S_2O_3^{2-}$ anions the disorder model of Table 2 proved to be most suitable. According to interatomic distance values between those of the S–S (2.01 Å) and S–O bonds (1.47 Å) in the isolated $S_2O_3^{2-}$ anion (Table 3) and the observed electron densities, the feature depicted in Fig. 4 may be interpreted as the superposition of eight different orientations of the $S_2O_3^{2-}$ anion with the statistical weights as given in Fig. 5. The position of the central atom is the only position which is always occupied by sulfur (S1). The highly anisotropic temperature factors of S1 and also of the O,S(3) and O,S(5) atoms (Fig. 4; see the U_{33} parameters in Table 4) indicate a slight

TABLE 3
Selected Bond Lengths (Å) and Bond Angles (°) in the Structure of $Na_8[Al_6Si_6O_{24}](S_2O_3) \cdot 2H_2O$

Al(1)–O(11)	1.733(8)	Al(2)–O(22)	1.722(7)
Al(1)–O(21)	1.735(8)	Al(2)–O(32)	1.751(10)
Al(1)–O(31)	1.719(10)	Al(2)–O(12)	1.731(8)
Al(1)–O(42)	1.762(9)	Al(2)–O(41)	1.745(8)
Average Al–O	1.736		
Si(1)–O(41)	1.613(9)	Si(2)–O(42)	1.612(9)
Si(1)–O(11)	1.611(8)	Si(2)–O(22)	1.610(7)
Si(1)–O(21)	1.620(8)	Si(2)–O(31)	1.637(9)
Si(1)–O(32)	1.613(8)	Si(2)–O(12)	1.613(8)
Average Si–O	1.618		
S(1)–S(2)/O(2)	1.70(2)		
S(1)–S(3)/O(3)	1.56(1)		
S(1)–S(4)/O(4)	1.78(3)		
S(1)–S(5)/O(5)	1.54(2)		
O(11)–Al(1)–O(21)	104.2(4)	O(22)–Al(2)–O(32)	113.0(4)
O(11)–Al(1)–O(31)	110.1(4)	O(22)–Al(2)–O(12)	107.2(4)
O(11)–Al(1)–O(42)	106.4(4)	O(22)–Al(2)–O(41)	114.3(4)
O(21)–Al(1)–O(31)	115.2(4)	O(32)–Al(2)–O(12)	109.4(4)
O(21)–Al(1)–O(42)	113.1(4)	O(32)–Al(2)–O(41)	105.7(4)
O(31)–Al(1)–O(42)	107.5(4)	O(12)–Al(2)–O(41)	106.9(4)
O(41)–Si(1)–O(11)	111.6(5)	O(42)–Si(2)–O(22)	111.0(5)
O(41)–Si(1)–O(21)	112.9(5)	O(42)–Si(2)–O(31)	107.5(4)
O(41)–Si(1)–O(32)	108.0(4)	O(42)–Si(2)–O(12)	109.9(4)
O(11)–Si(1)–O(21)	105.4(4)	O(22)–Si(2)–O(31)	112.0(4)
O(11)–Si(1)–O(32)	107.1(4)	O(22)–Si(2)–O(12)	108.7(4)
O(21)–Si(1)–O(32)	111.7(4)	O(31)–Si(2)–O(12)	107.7(4)
S(2)/O(2)–S(1)–S(3)/O(3)	116.4(5)	S(4)/O(4)–S(1)–S(5)/O(5)	114.7(5)
S(3)/O(3)–S(1)–S(3)/O(3)	101.8(5)	S(5)/O(5)–S(1)–S(5)/O(5)	103.7(5)

positional difference between the S1 centers in orientations 1,2 and 3,4, respectively (Fig. 5). The main contribution to the observed atomic occupancies of the disordered $S_2O_3^{2-}$ anion stems from orientations 1 (30%) and 4 (20%), implying that the axial S1–O,S bond along the channel axis has 50% "S–S" character. Hence, an interatomic distance intermediate between an S–S and S–O spacing (1.74 Å) is expected, in accord with the experimental values (Table 3). The three shorter bond lengths, on the other hand, should possess only about 17% S–S character (≃1.56 Å), which is again nicely confirmed by the experimental spacings. A similar orientational disorder is found

TABLE 4
Selected Anisotropic Temperature Parameters for the Thiosulfate Group in $Na_8[Al_6Si_6O_{24}](S_2O_3) \cdot 2H_2O$ ($\times 10^3$)

	U_{11}	U_{22}	U_{33}	U_{23}	U_{13}	U_{12}
S(1)	13(1)	13(1)	132(7)	0	0	6(1)
S,O(2); S,O(4)	44(3)	44(3)	56(10)	0	0	22(2)
S,O(3); S,O(5)	36(4)	69(6)	100(10)	−4(7)	−4(6)	37(4)

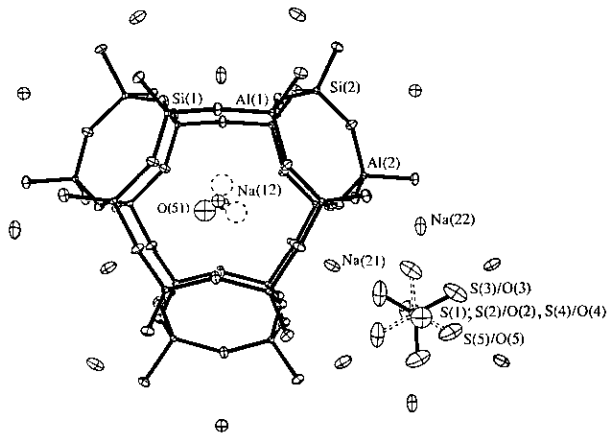

FIG. 3. View of the structure of $Na_8[Al_6Si_6O_{24}](S_2O_3) \cdot 2H_2O$ along the [001] direction, visualizing the disorder of the crystal water and of the thiosulfate anion.

in the case of sulfate anions incorporated into the cancrinite channels (10).

Good convergence of the refinement, performed against the F^2 data with the SHELXL-93 system (12), was obtained when using equal anisotropic temperature factors for all pairs of framework and sodium atoms related by the $P6_3$ pseudosymmetry. Similarly, the U_{ij} coefficients for the atom pairs (S,O)2/(S,O)4 and (O,S)3/(O,S)5, respectively, were set equal. The resulting residuals were $wR_2 = 0.076$ for all 1098 reflections, corresponding to a conventional $R = 0.0307$ for 1000 observed reflections [$I > 2\sigma(I)$]. A Flack x parameter of 0.10(8) indicates the probably correct orientation of the structure with respect to the polar axis. It should be noted that the effects of twinning and of the orientational disorder can be clearly differentiated because the twinning concerns the complete framework structure leading to an interchange of the Si and Al positions, for instance. The symmetry breaking induced by the $S_2O_3^{2-}$ groups has effects not so much on the framework as on the sodium positions within the large

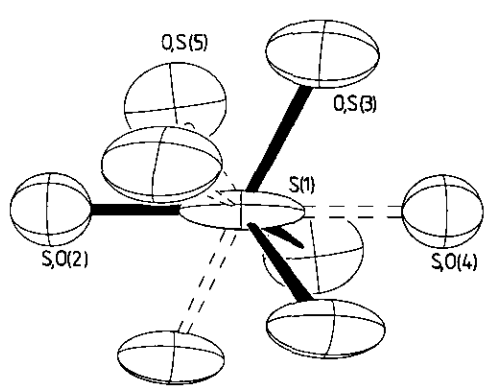

FIG. 4. The disordered thiosulfate group within the cancrinite channels (pseudo-S_6 ($\bar{3}$) axis parallel to the c unit cell axis).

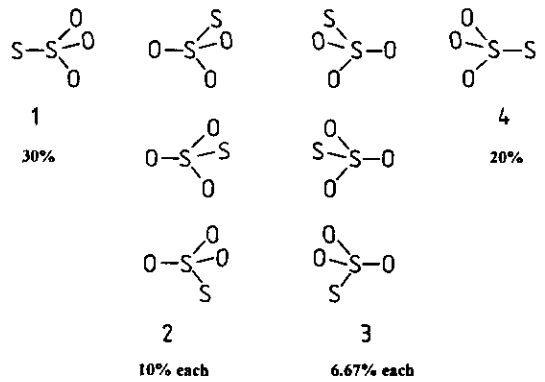

FIG. 5. The eight possible orientations of the thiosulfate anion. The percentage contributions to the feature in Fig. 4 are also given.

channels, which show parameter shifts up to 60 esd's from their ideal positions.

III.2. Irradiation and Thermal Treatment

ESR spectra of the colorless crystals revealed the presence of two radical species at very low concentrations, presumably SO_3^- (g = 2.0035) and S^- (g = 2.028). Reported g values for these species are g = 2.0035 and g = 2.031, respectively (14). UV/VIS spectroscopy reveals only one band with a maximum at 240 nm (41,700 cm^{-1}), which is due to lattice absorption. On irradiation with X-rays (e.g., Cu$K\alpha$) the thiosulfate cancrinite turns slightly yellow, generating an additional band at 406 nm (23,600 cm^{-1}) in the UV/VIS spectrum (Fig. 6) characteristic of the $^2\Pi_u \leftarrow {}^2\Pi_g$ transition of the S_2^- radical (1, 3, 15, 16). ESR spectra of the irradiated sample exhibit signals that are about three magnitudes of order more intense at the same positions as in the case of the untreated thiosulfate cancrinite (Fig. 7).

These results indicate a mechanism of S–S bond breaking in the $S_2O_3^{2-}$ anion, in which the S–S bonds are relatively weak in comparison with the bond strength in diatomic molecules (D^0_{298}/kJmol^{-1}: S–S 425; Al–O 508; S–O 522, Si–O 810 (17), with subsequent formation of S^- and SO_3^- fragments as well as S_2^-. The latter radicals are usually not detectable by ESR due to almost degenerate π-orbitals (2, 18). The formation of the above-mentioned radicals can be understood on the basis of the disorder of the thiosulfate group within the large channels of the cancrinite structure described before, namely by a cooperative mechanism involving one thiosulfate group with an "up" and the other with a "down" orientation [1]:

$$O_3S\text{–}S^{2-}\,(\text{up}) + S\text{–}SO_3^{2-}\,(\text{down}) \rightarrow O_3S^- + S_2^- + SO_3^{2-} \quad [1]$$

$$O_3S\text{–}S^{2-}\,(\text{up}) + O_3S\text{–}S^{2-}\,(\text{up}) \rightarrow O_3S^- + S^- + O_3S\text{–}S^{2-} \quad (\rightarrow O_3S^{2-} + S + O_3S\text{–}S^{2-}). \quad [2]$$

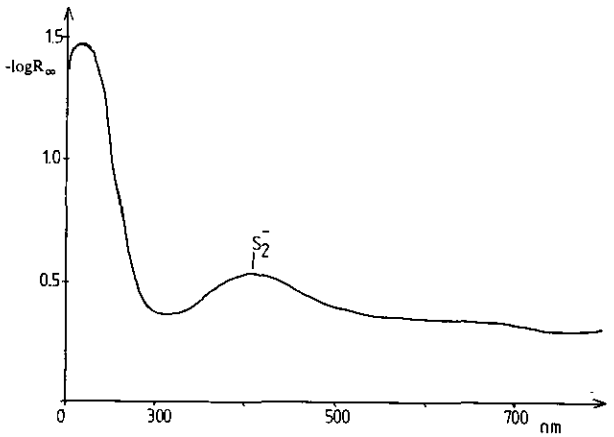

FIG. 6. UV/VIS spectrum of the thiosulfate cancrinite, irradiated by X rays (R_∞(diffuse reflectance) = $R_{sample}/R_{reference}$).

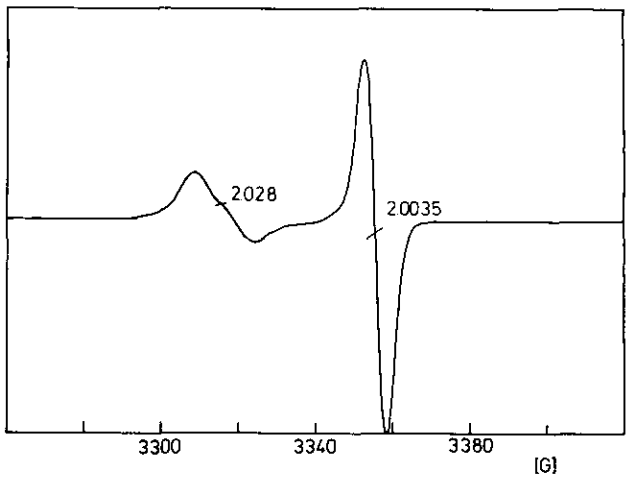

FIG. 7. ESR spectrum of the thiosulfate cancrinite, irradiated by X rays, measured at 9.409 GHz and 99 K.

In the case of only one orientation [2], a S or S^- fragment has to pass a $S_2O_3^{2-}$ anion or a $SO_3^{-(2-)}$ fragment, which, for reasons of available space, should be effectively hindered. No S_3^- radicals are generated by irradiation as indicated by ESR and UV/VIS spectroscopy.

If the thiosulfate cancrinite is treated thermally at 800°C in air or at 1000°C under flowing argon it turns via yellow and green colors to greenish-blue, without decomposition of the cancrinite framework. A UV/VIS spectrum of a greenish sample (800°C, air, 30 min) is shown in Fig. 8. S_2^- as well as S_3^- radicals can be identified by the shoulder around 400 nm (25,000 cm^{-1}) and the band at 595 nm (16,800 cm^{-1}) (1, 2, 16). The absorption around 300 nm could not be assigned. The EPR spectra only display the signal of the S_3^- radical (RT: $g \approx 2.03$; 103 K: g_x = 2.052, g_y = 2.035, g_z = 2.004), which, on comparison with g

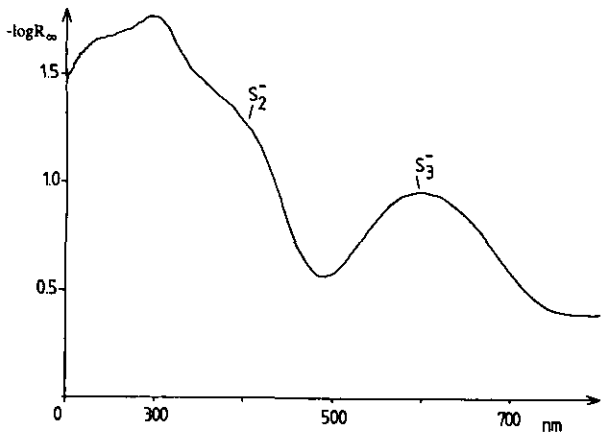

FIG. 8. UV/VIS spectrum of a thermally treated (30 min at 800°C in air) thiosulfate cancrinite.

values from literature (1, 2, 5, 14, 16, 19), can be definitely assigned.

In contrast to the processes during irradiation with X-rays the formation of triatomic radicals S_3^- can be understood by a thermally activated diffusive mechanism which allows the S/S^- fragments to migrate within the channels. We were not able to generate a purely blue color with exclusively S_3^- radicals, as Hund obtained in powder thiosulfate cancrinite samples (3), though we used a similar thermal treatment (1 hr, 1000°C, Ar stream). Heating for more than 1 hr led to a fading of the turquoise color.

ACKNOWLEDGMENTS

We owe thanks to Prof. Dr. E. Hoffer and H.-O. Brauer (mineralogical Institute, Marburg University), who offered help and the facilities for hydrothermal synthesis, and to Prof. Dr. R. Kniep and Mrs. V. Klink (Eduard Zintl Institut, Darmstadt) for performance of the SEM measurements. Financial support from the "Fonds der Chemischen Industrie" is gratefully acknowledged (G.-G. Lindner).

REFERENCES

1. F. Seel, *Stud. Inorg. Chem.* **5,** 67 (1984) and references therein.
2. G. G. Lindner, Thesis, Philipps University, Marburg, 1994; G. G. Lindner, D. Reinen, *Z. Anorg. Allg. Chem.* **620,** 1321 (1994).
3. F. Hund, *Z. Anorg. Allg. Chem.* **509,** 153 (1984).
4. R. M. Barrer, J. F. Cole, and H. Villinger, *J. Chem. Soc. A Inorg. Phys. Theor.*, 1523 (1970) and references therein.
5. J. Hassan and H. D. Grundy, *Can. Miner.* **27,** 165 (1989).
6. O. Jarchow, *Z. Kristallogr.* **122,** 407 (1965).
7. K.-H. Klaska and O. Jarchow, *Naturwissenschaften* **64,** 93 (1977).
8. R. Rinaldi and H.-R. Wenk, *Acta Crystallogr. Sect. A* **35,** 825 (1979).
9. N. B. Pahor, M. Calligaris, G. Nardin, and L. Randaccio, *Acta Crystallogr. Sect. B* **38,** 893 (1982).
10. I. Hassan and H. D. Grundy, *Can. Miner.* **22,** 333 (1984).
11. H. D. Grundi and I. Hassan, *Can. Miner.* **20,** 239 (1982).
12. G. M. Sheldrick, "SHELXL-93, Program for the Refinement of Crystal Structures." Universität Göttingen, 1993.
13. D. T. Cromer and J. T. Waber, *in* "International Tables for Crystallography," Vol. C, Tables 6.1.1.4 and 4.2.6.8, Kluwer Academic, Dordrecht, 1992.
14. K. M. Hellwege and A. M. Hellwege, (Eds.) "Landolt-Boernstein Numerical Data and Functional Relationships in Science and Technology. New Series, Group 2: Atomic and Molecular Physics," Vol. 9a. Springer-Verlag, Berlin/New York, 1977 and references therein.
15. R. J. H. Clark and D. G. Cobbold, *Inorg. Chem.* **17,** 3169 (1978).
16. F. Seel, H.-J. Güttler, A. B. Wieçkowski, and B. Wolf, *Z. Naturforsch. B* **34,** 1671 (1979).
17. R. C. Weast (Ed.), "Handbook of Chemistry and Physics," 66th ed. CRC Press, Boca Raton, FL, 1985–1986.
18. J. A. Rabo, "Zeolite Chemistry and Catalysis, Am. Chem. Soc., Washington, DC." ACS Monograph 171, p. 80. 1976.
19. J. Schneider *et al., Phys. Status Solidi* **13,** 141 (1966).